Contents lists available at ScienceDirect

Carbon

journal homepage: www.elsevier.com/locate/carbon

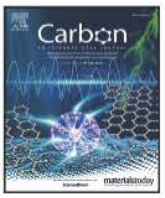

Highlights

**3D nanostructure prediction of porous carbons via gas adsorption**

*Carbon xxx (xxxx) xxx*

Fernando Vallejos-Burgos*, Carla de Tomas, Nicholas J. Corrente, Koki Urita, Shuwen Wang, Chiharu Urita, Isamu Moriguchi, Irene Suarez-Martinez, Nigel Marks, Matthew H. Krohn, Radovan Kukobat, Alexander V. Neimark, Yury Gogotsi, Katsumi Kaneko

- New 3D-VIS procedure to obtain morphological parameters of nanocarbons.
- Realistic kernel and script obtained via molecular dynamics is provided.
- 3D-VIS predicts plausible 3D structure, PSD, area and adsorption of other molecules.

Contents lists available at ScienceDirect

Carbon

journal homepage: www.elsevier.com/locate/carbon

Graphical Abstract

**3D nanostructure prediction of porous carbons via gas adsorption**

*Carbon xxx (xxxx) xxx*

Fernando Vallejos-Burgos*, Carla de Tomas, Nicholas J. Corrente, Koki Urita, Shuwen Wang, Chiharu Urita, Isamu Moriguchi, Irene Suarez-Martinez, Nigel Marks, Matthew H. Krohn, Radovan Kukobat, Alexander V. Neimark, Yury Gogotsi, Katsumi Kaneko

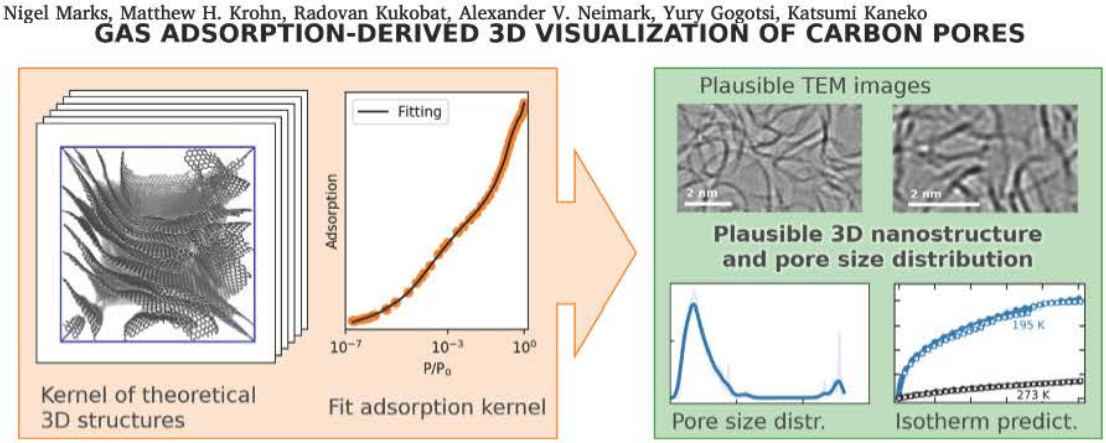

Contents lists available at ScienceDirect

Carbon

journal homepage: www.elsevier.com/locate/carbon

Research article

# 3D nanostructure prediction of porous carbons via gas adsorption

Fernando Vallejos-Burgos [a,b,*], Carla de Tomas [c], Nicholas J. Corrente [d], Koki Urita [e], Shuwen Wang [b], Chiharu Urita [e], Isamu Moriguchi [e], Irene Suarez-Martinez [f], Nigel Marks [f], Matthew H. Krohn [a], Radovan Kukobat [g], Alexander V. Neimark [d], Yury Gogotsi [h], Katsumi Kaneko [b]

[a] Morgan Advanced Materials, Carbon Science Centre of Excellence, 310 Innovation Blvd. Ste 250, State College, PA 16803, USA
[b] Research Initiative for Supra-Materials, Shinshu University, Nagano, 380-8553, Japan
[c] Department of Chemical Engineering, Imperial College London, London, SW7 2BX, UK
[d] Department of Chemical and Biochemical Engineering, Rutgers, The State University of New Jersey, Piscataway, NJ 08854, USA
[e] Graduate School of Engineering, Nagasaki University, Nagasaki, 852-8521, Japan
[f] Department of Physics and Astronomy, Curtin University, Perth, 6102, WA, Australia
[g] Department of Chemical Engineering and Technology, University of Banja Luka, Banja Luka, 78000, Bosnia and Herzegovina
[h] A.J. Drexel Nanomaterials Institute and Department of Materials Science and Engineering, Drexel University, Philadelphia, PA 19104, USA

ARTICLE INFO

*Keywords:*
Gas adsorption
Nanoporous carbons
Surface area
Pore size distribution
Adsorption prediction
Nanoscale imaging

ABSTRACT

Structural characterization of porous carbon materials is critical for the evaluation of their synthesis procedures and performance. Throughout the last decades, many methods have been employed to determine porosity properties from gas adsorption such as surface area, pore size distribution (PSD) and real density. However, gas adsorption models use 1D structures of carbon nanopores, although adsorption and separation properties of nanoporous carbons are governed by 3D pore parameters. Estimating the 3D nanostructure of nanoporous carbons using gas adsorption would accelerate progress in research and implementation of nanoporous carbons. We report here a promising 3D pore nanostructural characterization from gas adsorption. Using atomistic simulations, we have generated a database of realistic 3D porous carbon structures spanning a wide range of pore sizes and geometries. After calculating their gas adsorption isotherms, we employed a numerical procedure to find the relative contribution for each of the structures to the adsorption isotherm of a nanoporous carbon sample. These contributions allowed us to estimate the surface area and pore size distribution of carbon materials; moreover (and perhaps more importantly!), we will show that the plausible 3D pore structures correlate very well with the local carbon structure as experimentally determined by high-resolution TEM observations and can successfully predict adsorption of different molecules. This is a powerful procedure that can be extended to other materials, and with enough computer power, to larger pore sizes.

## 1. Introduction

Nanoporous carbons have been developed for energy storage applications due to high surface area and porosity, high electrical conductivity, high thermal conductivity, and chemical robustness [1,2]. Nanoporous carbons are accessible to adsorbate molecules, being promising for batteries, supercapacitors, membranes, and catalysts [2]. Wide range of applications of nanoporous carbons arises from its structure and porosity. Thus, accurate evaluation of pore structure and porosity using classical one-dimensional values such as average pore size ($w$) and pore size distribution (PSD) is mandatory for screening promising nanoporous carbons. IUPAC classifies nanopores into micropores (< 2 nm), mesopores (2 nm to 50 nm), and macropores (> 50 nm) using the one-dimensional parameter $w$ [3]. However, real nanopores are 3D structured, which determine the dynamic behavior of molecules and/or ions in the nanopores. High performance nanoporous carbons

* Corresponding author at: Morgan Advanced Materials, Carbon Science Centre of Excellence, 310 Innovation Blvd. Ste 250, State College, PA 16803, USA.
*E-mail addresses:* fvb@vallejos.cl (F. Vallejos-Burgos), c.detomas@imperial.ac.uk (C. de Tomas), nicholas.corrente@rutgers.edu (N.J. Corrente), urita@nagasaki-u.ac.jp (K. Urita), s_wang@shinshu-u.ac.jp (S. Wang), curita@nagasaki-u.ac.jp (C. Urita), mrgch@nagasaki-u.ac.jp (I. Moriguchi), I.Suarez-Martinez@curtin.edu.au (I. Suarez-Martinez), N.Marks@curtin.edu.au (N. Marks), Matthew.Krohn@morganplc.com (M.H. Krohn), radovan.kukobat@tf.unibl.org (R. Kukobat), aneimark@rutgers.edu (A.V. Neimark), gogotsi@drexel.edu (Y. Gogotsi), kkaneko@shinshu-u.ac.jp (K. Kaneko).

https://doi.org/10.1016/j.carbon.2023.118431
Received 28 April 2023; Received in revised form 23 August 2023; Accepted 30 August 2023

are necessary for enhancement of storage and reaction of molecules and/or ions. The 3D visualization of nanopores of carbon is the key to accelerating the storage of renewable energies and utilization of $CO_2$. A simple evaluation method of 3D visualization of carbon nanopores can contribute to better understanding the pore structure and porosity. If we determine the 3D pore structure together with the PSD of a target nanoporous carbon from gas adsorption, such as $N_2$ adsorption at 77 K, we can predict the diffusion, adsorption, and catalysis through computer simulation in advance, giving rise to the progress in development of the optimum nanoporous carbon structures.

The critical component of the method for determination of the nanoporous structure in real carbon samples is the modeling of the pores. In the conceptual approach, the simplest and the most widely used is the slit pore model [4], where the pore is defined as the space between two semi-infinite parallel graphitic layers. Further refinements included pores of different geometries [5–10], as well as introduction of defects on the original slit pore model and its variations, and construction of pore network with slit pores of different sizes and orientations [11–13]. Slit and cylindrical pore models are currently the most advanced ways to characterize the adsorption properties of nanoporous carbons experimentally via approaches based on density-functional theory (DFT), starting with the application of non-local DFT theory (NLDFT [14]) to characterize porous carbons and later developing into quenched-solid DFT (QSDFT [15]) and 2D-NLDFT [16]; all of these were commercially implemented. However, these models are still highly idealized and neglect important features of the real porous networks by treating the atomistic nature of the porous structure as a geometric space, losing effects such as curvature, percolation, internal edges and heterogeneous pore sizes and shapes distributions, all which lead to computational artifacts in the PSD [17].

Simulated models of nanoporous carbon structures are more realistic than conceptual models. They generate the porous networks via an interatomic potential and are able to reconstruct the atomic coordinates using experimental data via hybrid reverse Monte Carlo (HRMC [18,19]) or by mimicking the laboratory synthesis process via molecular dynamics (MD [20–22]). In a previous work, we performed MD simulations with EDIP [23] to mimic the synthesis of carbide-derived carbons [24]. This simulation method depends only on annealing temperature and material density, resulting in realistic porous carbon networks featuring different pore sizes and geometries, including slit-like, conic-like, cylindrical-like shapes. The networks are 3D-connected and percolated, with graphenic pore walls of different degree of purity, containing structural defects such as vacancies, $sp^3$ cross-links, and internal edges. Characterization of a number of porous carbons using our method agreed well with experimental characterization, including adsorption properties, X-ray diffraction and radial distribution function, and mechanical properties [24–28]. Our previous models were also incorporated to the porous carbons database [29], and employed to further characterize adsorption properties of commercial activated carbons [30].

This successful validation of our modeling method motivated us to build an extensive collection of realistic porous carbon structures systematically spanning a wide range of porosity and graphenization/graphitization degrees, from narrow micropores to small mesopores. From this we build a kernel of adsorption isotherms which serves as the basis for the development of a novel and so far the most realistic carbon nanostructure characterization method, which we denote as 3D-VIS due to its novel visualization capability. Our 3D-VIS method employs atomistic structure coordinates which do not require fitting of model parameters to experimental reference isotherms, contrary to current DFT-based methods. Our method is validated against experimental samples (carbide-derived carbons and industrially-relevant activated carbons), providing more accurate results than commercial DFT-based methods. 3D-VIS is integrated into a user-friendly script which provides a simple and ready-to-use tool for the wide community to characterize their nanoporous carbons by obtaining plausible 3D geometries, PSDs and textural parameters.

## 2. Summarized methodology

We present a nanoporous carbon characterization method that finds plausible 3D structures and morphological parameters via fitting its experimental gas adsorption isotherm.

More specifically, the procedure (see Fig. 1) is to first generate a series of realistically-simulated carbon structures through molecular dynamics (MD) using various combinations of annealing (graphitization) temperatures and densities to cover a wide range of nanoporous carbons. These structures are cartesian coordinates for carbon atoms. After generating the structures, we calculated their $N_2$ adsorption isotherms via grand canonical Monte Carlo (GCMC) simulations, and corresponding morphological parameters including PSD, surface area, and pore volume. The adsorption isotherms were stored into a PSD kernel. For consistency with larger pore sizes, a dozen structures were added with pores larger than those practically feasible in our simulations by using a mesopore model based on the Kelvin equation [31] allowing us to reach up to 40 nm; beyond this range the nanostructure does not have relevance in the features of the isotherm, except its magnitude.

By finding a linear combination of isotherms of our kernel that can reproduce the experimentally measured isotherm, it is possible to calculate the morphological (or textural) parameters of the experimental sample together with a plausible simulated HR-TEM image.

Our structures are generated via annealed molecular dynamics and have been extensively characterized and validated through comparison with experimental data, including coordination fractions, g(r), TEM, XRD, mechanical and adsorption properties [24–28,32,33]. The full methodology is described in detail in Supporting Information S1 and an online open repository stores all relevant data [34].

At this initial stage we have provided an isotherms kernel of $N_2$ adsorption at 77 K which due to the phenomenological nature of adsorption in carbon cannot recreate every isotherm type. It is worth noticing however that the method itself is not limited to this kernel and more can be developed in a similar manner. The current status for all isotherm types is then: (i) For an isotherm type I the method and kernel provided works especially well for since these describe a microporous structure for the length scale of the developed kernel. (ii) For an isotherm type II the method also works well as long as the correction for a non-porous sample is provided as in this case. (iii) The $N_2$ kernel provided does not accommodate type III isotherms in nanocarbons due to the relatively weak adsorbate–adsorbent affinity. To account for Type III isotherms, the GCMC isotherms must be recalculated for the adsorbate using the same structures and, for example, using $H_2O$ as adsorbent. This can be implemented in future iterations of this work. (iv) Type IV isotherm can be implemented with a correction. In the atomic length scale where the structures were synthesized via molecular dynamics, it is not computationally-feasible to include mesopores (yet), however in these pores the nanostructure is not relevant. In this work we included a correction to consider mesopores via the Kelvin equation. (v) Type V isotherms can also be implemented with a correction and a new kernel since the phenomenon is a combination of a type III and type IV isotherms. (vi) Type VI is also feasible. However it would require measurement of the GCMC kernel at conditions in which a type VI isotherm is formed. Some of our structures (see for example #64) possess only a single step since several well-marked steps do not occur for $N_2$ at 77 K. This can be implemented in future iterations of this work.

## 3. Results and discussion

### 3.1. Simulated porous carbon structures database

Systematic variation of simulation temperature and density gives nanoporous carbon structures with variable degree of porosity, short-range order and graphenization/graphitization, as demonstrated in our previous study [24,25]. We identify four stages during nanoporous

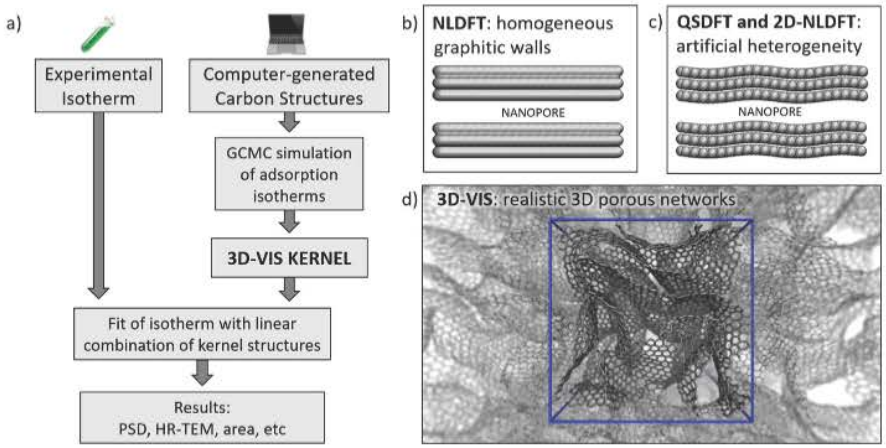


**Fig. 1.** (a) General scheme of the 3D-VIS method. We create a kernel of realistic computer-generated carbon structures and determine their adsorption and textural properties. The contribution of each kernel structure, fitting the experimental adsorption isotherm was found through numerical methods from the known properties of the kernel and the experimental isotherms. (b) Pore models employed in NLDFT at the pore sizes defined by the separation between two infinite graphitic slabs. (c) QSDFT and 2D-NLDFT include corrugation and heterogeneity of the surface. (d) Example of a 3D porous network model employed in our 3D-VIS method, showing coexistence of pores with different sizes, geometries, having defects and curvatures. The periodic simulation box is highlighted in blue.

structure generation: (i) low annealing temperatures and low densities result in highly amorphous and microporous carbons, with no graphitic nanodomains, *i.e.*, no slit-shaped pores. The high degree of disorder in this regime is quantified via ring statistics and coordination fractions, where large number of non-hexagonal rings and significant fractions of $sp$ and $sp^3$-hybridized atoms were observed; (ii) high annealing temperature and low densities provide a different sort of porous carbons, and the higher temperature drives short-range order rearrangements. This rearrangement results in larger and more graphenic pore walls, having less defects as indicated by a predominant number of hexagons, and above *ca.* 90% of $sp^2$ hybridized atoms on average. Temperature-driven rearrangement imposes the development of mesopores due to low density, as observed at the structures whose density was $0.10\,g\,cm^{-3}$ to $0.25\,g\,cm^{-3}$; (iii) low temperature and high densities as reminiscent of the structure of coal [35,36]; (iv) high temperatures and high densities impose significant graphitization and abundance of slit-shaped pores interconnected with narrow micropores, being typical for hard carbons in the density range of $1.0\,g\,cm^{-3}$ to $1.5\,g\,cm^{-3}$. Structures calculated at the densities below $0.10\,g\,cm^{-3}$ were not annealed into continuous frameworks and were thereby removed from the kernel. These structures were more alike a molecule than a solid.

Not unexpectedly, the pore sizes of the generated structures are found to be strongly dependent on their density since the mean pore size, as calculated from the first momentum of PSD, decreased exponentially with increasing density (see Fig. S1a). The total surface area (see Fig. S1b) exceeded that of graphene for densities below $0.50\,g\,cm^{-3}$ due to a low stacking and high ratio of carbon at the edges against the basal plane, decreasing linearly with density. On the other hand, there was no clear correlation between the pore size and the simulation temperature (see Fig. S1c).

It is worth noting that real carbon structures exhibit a variety of functional groups [37], which are not explicitly present in our carbon structures composed by the carbon atom only. Nevertheless, these functionalities only play a secondary role as compared to porosity [38], as demonstrated theoretically and experimentally through heat of adsorption measurements. The main advantage of our proposed approach is in creating a representative set of carbon structures annealed at different temperatures to cover a wide practical temperature–density area of interest. These structures are inherently heterogeneous with varying pore wall curvature, presence of Stone–Thrower–Wales defects, and carbon edges.

**Table 1**
Textural characteristics of the porous carbons tested as analyzed by classical methods and 3D-VIS.

| Sample | Surface area ($m^2/g$) | | Pore volume ($cm^3/g$) | |
|---|---|---|---|---|
| name | BET[a] | 3D-VIS | Experimental[b] | 3D-VIS |
| CDC-400 | 1144 | 986 | 0.53 | 0.55 |
| AC-YP50F | 1556 | 1378 | 0.79 | 0.74 |
| ACF-A20 | 1671 | 1716 | 1.13 | 1.10 |
| PG-600 | 1162 | 1129 | 0.75 | 0.71 |

[a] Pressure range calculated according to Rouquerol [43] criteria.
[b] Pore volume calculated at $P/P_0 = 0.99$.

### 3.2. Characterization of experimental carbon samples

We studied the $N_2$ adsorption isotherms of four representative nanoporous carbons: a carbide derived carbon produced by extracting Ti from TiC [39] at 400 °C (CDC-400), an industrially relevant activated carbon (AC-YP50F) [40], an activated carbon fiber (ACF-A20) [41], and a porous graphene (PG-600) [42]. These nanoporous carbons showed an evident isotherm type-I behavior [3] characteristic of microporous carbons (see Fig. S3a,b). They also exhibited medium to high surface area and a moderate pore volume (see Table 1).

BET theory has a long and successful history for porosity evaluation. While it is well known that the BET method is unsatisfactory to evaluate total surface areas [44] and often overestimates their values [45], it is still the most widely used method for surface area evaluation due to its simplicity. However, when this method is applied to adsorbents whose isotherms are unable to satisfy the BET assumptions, more sophisticated criteria are required for porosity assessment, which complicate the applicability of this method [46]. Furthermore, the imperfect and insufficient manual calculations cause low reproducibility [44]. Advanced mathematical evaluation methods based on DFT theory have contributed to understand porous carbons. However, further improvements of the DFT method are needed for reliable porosity characterization.

The 3D-VIS model shows an excellent fit of the nanoporous carbons employed in this study (see Fig. 2). The fit follows the different curvatures observed in the experimental nanoporous carbons. The residual errors deviate from the experimental points by ~ 1%. A somewhat larger difference usually occurs at the relative pressure region below

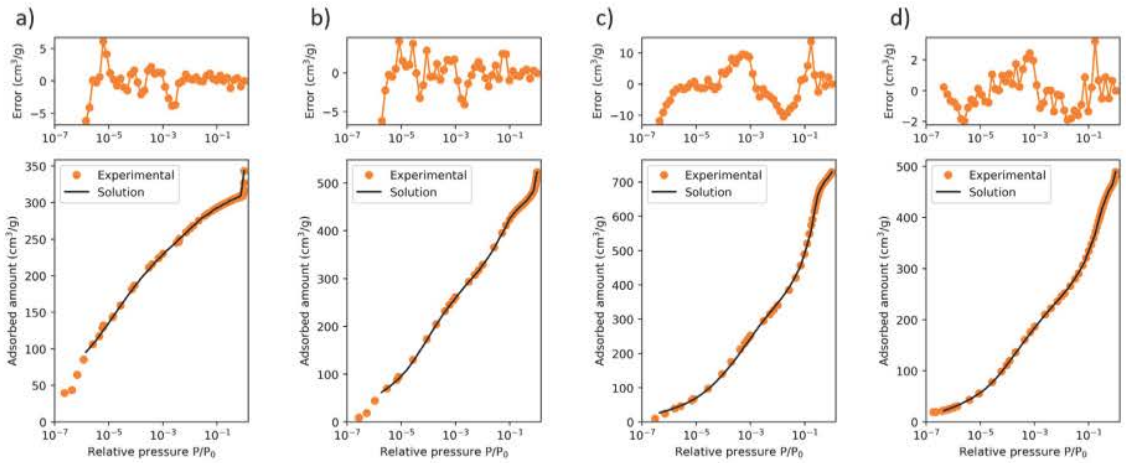


**Fig. 2.** Experimental $N_2$ adsorption isotherms plotted with the fit of the 3D-VIS model. (a) CDC-400, (b) AC-YP50F, (c) ACF-A20 and (d) PG-600.

$10^{-5}$ where the experimental measurements are uncertain [47]. However, since the residual errors are still not random, we expect the fit to improve in future iterations of this work by adding more structures to the kernel.

The BET surface areas of CDC-400 and AC-YP50F are ~ 15% larger than their 3D-VIS counterparts, while those of ACF-A20 and PG-600 almost coincide with the results from 3D-VIS. The difference between BET and 3D-VIS methods for narrow micropores is attributed the over-simplified assumptions applied in the BET equation, including monolayer formation, no interaction between adsorbed molecules, uniform adsorbate coverage, and hexagonal close-packing. The pore volumes of these four carbons determined from Gurvitch's rule and 3D-VIS method differ by 3%–7%, showing good reliability of these methods. Nevertheless, the porosity of microporous carbons determined from conventional methods and the 3D-VIS method show quite good consistency.

### 3.3. TEM comparison

We observed nanoporous carbon structures experimentally with TEM and simulated the TEM micrographs for validation of our method. Considering the number of graphene layers, the carbon structures can be classified into a few layer and multi-layer structures. CDC-400 has a few layer structure, consisting of densely packed graphene with edges that represent the pore walls (see Fig. 3). AC-YP50F, ACF-A20, and PG-600 form layered structures that are not closely packed. We can observe similarities between the simulated TEM images and experimentally observed carbon structures, showing the reliability of our approach. Predicted structures #24 and #71 significantly contribute to the CDC-400 model. The TEM images were focused on the edge area of the particles for clear observation of the carbon structures. The layered structure group is additionally classified according to the two dimensional size of each layer. AC-YP50F has densely packed structure of wavy layers, while ACF-A20 and PG-600 has layer structures of flat graphenes. Both samples have high contribution to the layered structures. Nanoporous carbon models that contribute to the $N_2$ adsorption isotherms at 77 K correspond to the TEM simulated structures. In addition, we compare the pore sizes estimated from the TEM images and calculated pore sizes to clarify our method. CDC-400 has a narrow PSD distribution of ~0.8 nm, AC-YP50F and ACF-A20 have a wide pore size distributions of ~0–3 nm, while PG-600 has a bit wider pore size distribution of ~0–4 nm (Fig. 4). The narrow pores of CDC-400 arise from the densely shrinked graphene-like structure, forming narrow pores (see Fig. 3). On the other hand, AC-YP50F, PG-600 and ACF-A20 consist of graphene layers that are not densely packed, giving wider pores than that of CDC-400. The pore sizes between the observed pores and the calculated ones are similar, suggesting the reliability of the 3D PSD method.

### 3.4. Pore size distribution (PSD)

We calculated PSD of four samples using 3D-VIS method developed in this work and modern DFT including QSDFT, NLDFT, and 2D-NLDFT for comparison (see Fig. 4). As expected, the simplest NLDFT method shows a singularity at 0.8 nm, corresponding to a layering transition artifact [15] due to the monolayer transition in smooth graphite inherent to this method. The artifact behavior was slightly corrected by adding a roughness factor to the pore wall in QSDFT. Yet, the sharp peaks and zeros can be observed in the PSD plots [48,49]. 2D-NLDFT provides a more physically-plausible PSD using energetic heterogeneity and geometrical corrugation, removing most of the artifacts in the PSD plot. The DFT methods cannot take into account realistic features of the carbon structure such as curvature and pore length due to slit- or cylinder-shaped pores [50]. Resolving these issues require complex approaches such as combining DFT models and adsorbates [48,49], or coupling with additional methods to evaluate porosity [51].

In contrast, our 3D-VIS method does not require additional fitting to remove artifacts because each simulated nanocarbon structure has common defects, uneven pore spacing, and curvatures. These features were implemented in the calculation process, resulting in artifact-free PSD curves.

### 3.5. Prediction of $CO_2$ adsorption

$CO_2$ adsorption at 273 K is a popular alternative to $N_2$ adsorption at 77 K for porosity evaluation [52,53]. Although the $CO_2$ molecule is unsuitable for characterization of polar materials due to its strong quadrupole moment, it shows great advantage for non-polar materials containing narrow micropores whose $N_2$ adsorption is hardly measurable at 77 K due to extremely slow diffusivity. $CO_2$ at 273 K diffuses much faster than $N_2$ at 77 K, penetrating into narrow pores and allowing reliable evaluation of porosity parameters. We compare the experimentally measured and predicted $CO_2$ isotherms at 195 K and 273 K (see Fig. 5). The predicted isotherms were calculated from the same structure contribution found in the solution of the $N_2$ isotherms at 77 K. The isotherms at 273 K show similarity, suggesting the feasibility for predicting $CO_2$ adsorption in narrow micropores. Note that at

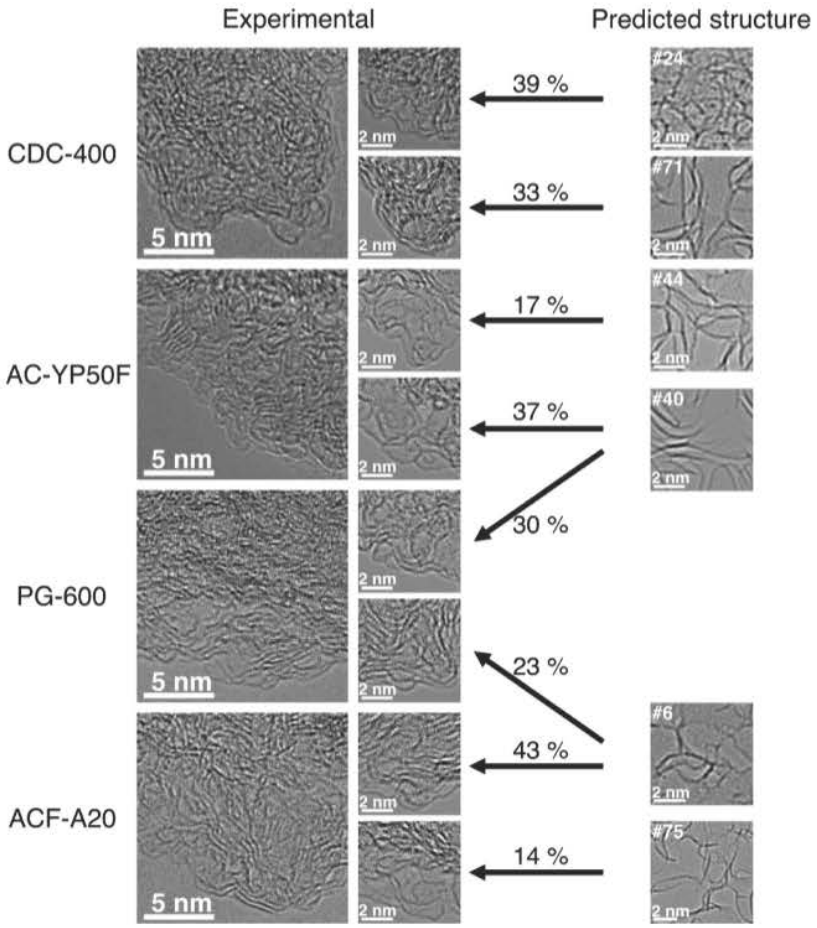


**Fig. 3.** Comparison of TEM images between experimental samples and carbon models. Carbon models that contributed the most to the adsorption isotherm fit are shown as simulated TEM images.

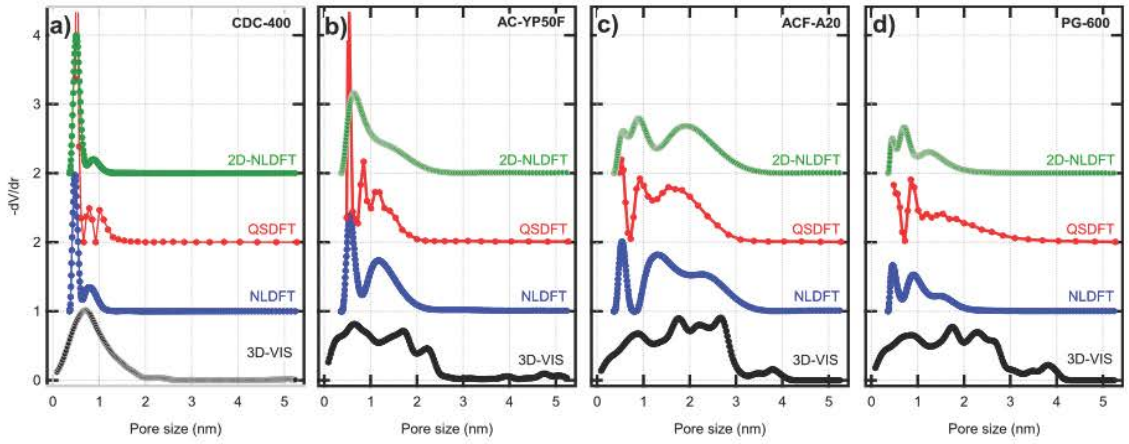


**Fig. 4.** Comparison of pore size distributions calculated with 3D-VIS and DFT methods: (a) CDC-400, (b) AC-YP50F, (c) ACF-A20, and (d) PG-600.

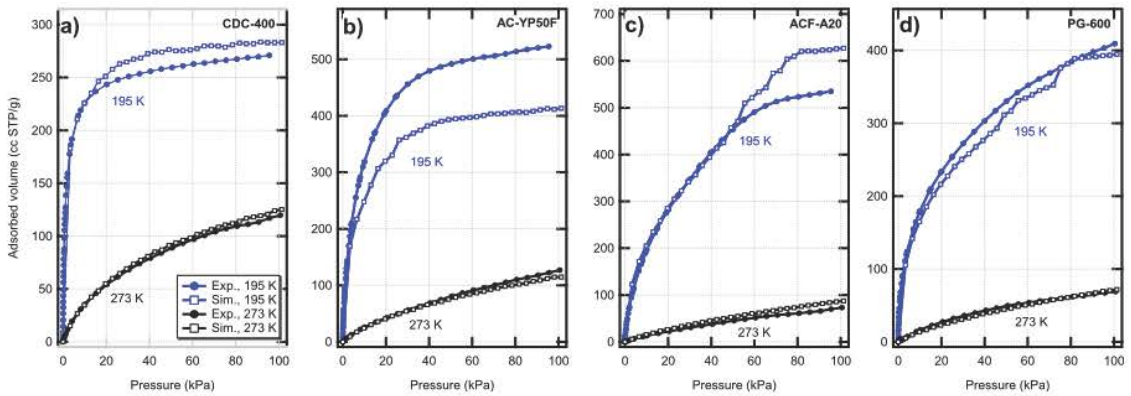


**Fig. 5.** Comparison of experimentally measured and predicted $CO_2$ adsorption for relevant microporous carbons: (a) CDC-400, (b) AC-YP50F, (c) ACF-A20, and (d) PG-600. Isotherms predicted and then measured at 273 K show excellent agreement.

273 K, the range of pores filled by $CO_2$ at sub-atmospheric pressures is limited by ~1 nm [54]. At 195 K, the simulated isotherms agree with the experimental isotherms at low pressures, corresponding to narrow micropore filling. In contrary, the isotherms slightly deviate in the region of wider micro/mesopore filling at $P/P_0 > 0.2$. These deviations may be related to the surface chemistry of adsorbents that does not capture $N_2$, *e.g.*, $N_2$ has quadrupole moment which interacts weakly with polar functional groups at carbon surface, while $CO_2$ is sensitive to polar functional groups on carbon surface due to its three times stronger quadrupole moment [55]. Another factors are the limited size of 3D models and periodic boundary conditions employed in GCMC simulations.

## 4. Conclusion and outlook

We have developed a nanoporous carbon characterization method (3D-VIS) based on gas adsorption isotherms. 3D-VIS method can provide a plausible and realistic 3D-nanostructure of nanoporous carbons, predicting adsorption isotherms of molecules, giving surface area, pore size distribution, and porosity parameters.

More specifically, a database kernel of 78 carbon structures simulated through molecular dynamics provides a wide range of morphological characteristics in both synthesis temperature and density, which are able to fit the $N_2$ isotherm of a given experimental carbon. The weights of the fit show the most likely structures that behave as the experimental carbon. It is worth noting that the method is general and not limited to $N_2$ adsorption since new kernels can be developed in a similar manner.

The method was tested on four commercially interested nanoporous carbons: carbide derived carbon, active carbon for Li-ion batteries, activated carbon fibers, and porous graphene.

As with every method, 3D-VIS also has its shortcomings: (i) it is indeed computationally-demanding to synthesize and simulate very large structures, and thereby we limited our structure to 5.5 nm in size. Although we considered the top limit of mesopores (40 nm) by hybridizing our method with Kelvin's equation appropriate for mesopores, we expect that the regular advances in computer power will eventually overcome this limitation. (ii) No surface chemistry and/or charges were included in the provided kernel. However this has been the norm for DFT-based method, and in the case of 3D-VIS it can be overcome by simulating more structures and adding typical surface groups found in carbons.

This is evidently the most advanced method to obtain characteristics of carbons only from their adsorption isotherms. The prediction of all pore size distribution, gas adsorption and plausible 3D structures will be an invaluable help in study and understanding of nanoporous carbon structures in a more realistic way.

## CRediT authorship contribution statement

**Fernando Vallejos-Burgos:** Conceptualization, Methodology, Software, Investigation, Writing – original draft, Visualization, Project administration. **Carla de Tomas:** Methodology, Formal analysis, Investigation, Writing – original draft. **Nicholas J. Corrente:** Validation, Formal analysis, Investigation. **Koki Urita:** Validation, Investigation, Visualization, Writing – original draft. **Shuwen Wang:** Formal analysis, Investigation, Validation, Writing – original draft. **Chiharu Urita:** Investigation. **Isamu Moriguchi:** Resources. **Irene Suarez-Martinez:** Methodology. **Nigel Marks:** Conceptualization, Resources, Writing – original draft. **Matthew H. Krohn:** Software. **Radovan Kukobat:** Writing – original draft. **Alexander V. Neimark:** Methodology, Resources, Supervision. **Yury Gogotsi:** Resources. **Katsumi Kaneko:** Methodology, Resources, Supervision, Writing – original draft.

## Declaration of competing interest

The authors declare the following financial interests/personal relationships which may be considered as potential competing interests: Carla de Tomas reports financial support was provided by EU Horizon 2020 RD Programme Marie Sklodowska-Curie grant 101025294. Nicholas Corrente reports financial support was provided by NSF CBET grant No 1834339. Alex Neimark reports financial support was provided by NSF CBET grant No 1834339. Katsumi Kaneko reports financial support was provided by Japan Science Technology Agency (JST) Open Innovation Platform with Enterprise, Research Institute and Academia (OPERA)- (JPMJOP1722) and Kotobuki Holdings Ltd.

## Acknowledgments

The authors thank Prof. Alexander Puziy for gently providing KAUm sample used in the initial stages of this study and Prof. Dr. Martin Fierz for providing NNLS computer routines for LabVIEW. C.d.T. acknowledges funding from the European Union's Horizon 2020 research and innovation programme under the Marie Sklodowska-Curie grant agreement No. 101025294. N.C. and A.N. acknowledge NSF CBET grant No 1834339. K.K. acknowledges Japan Science Technology Agency (JST) Open Innovation Platform with Enterprise, Research Institute and Academia (OPERA)- (JPMJOP1722) and Kotobuki Holdings Ltd.

## Appendix A. Supplementary data

Supplementary material related to this article can be found online at https://doi.org/10.1016/j.carbon.2023.118431.

1. Detailed methodology and supporting figures.

2. Detailed information and results for every model structure in the kernel.

3. Spreadsheet summary with model results including adsorption isotherms and PSDs.

4. Jupyter script to process experimental adsorption isotherm and obtain plausible TEM images, PSD and textural parameters all available in the online repository [34].

## References


[1] G. Sneddon, A. Greenaway, H.H.P. Yiu, The potential applications of nanoporous materials for the Adsorption, Separation, and Catalytic Conversion of Carbon Dioxide, Adv. Energy Mater. 4 (10) (2014) 1301873.

[2] V. Meunier, C. Ania, A. Bianco, Y. Chen, G.B. Choi, Y.A. Kim, N. Koratkar, C. Liu, J.M.D. Tascon, M. Terrones, Carbon science perspective in 2022: Current research and future challenges, Carbon 195 (2022) 272–291.

[3] M. Thommes, K. Kaneko, A.V. Neimark, J.P. Olivier, F. Rodriguez-Reinoso, J. Rouquerol, K.S.W. Sing, Physisorption of gases, with special reference to the evaluation of surface area and pore size distribution (IUPAC Technical Report), Pure Appl. Chem. 87 (9–10) (2015) 1051–1069, Publisher: De Gruyter.

[4] P.H. Emmett, Adsorption and Pore-Size Measurements on Charcoals and Whetlerites, Chem. Rev. 43 (1) (1948) 69–148.

[5] Y. Zeng, P. Phadungbut, D.D. Do, D. Nicholson, Wedge Pore Model as an Alternative to the Uniform Slit Pore Model for the Determination of Pore Size Distribution in Activated Carbon, J. Phys. Chem. C 119 (46) (2015) 25853–25859.

[6] Q.K. Loi, L. Prasetyo, J.S. Tan, D.D. Do, D. Nicholson, Wedge pore modelling of gas adsorption in activated carbon: Consistent pore size distributions, Carbon 166 (2020) 414–426.

[7] I. Cabria, M.J. López, J.A. Alonso, Simulation of the hydrogen storage in nanoporous carbons with different pore shapes, Int. J. Hydrogen Energy 36 (17) (2011) 10748–10759.

[8] G.Y. Gor, M. Thommes, K.A. Cychosz, A.V. Neimark, Quenched solid density functional theory method for characterization of mesoporous carbons by nitrogen adsorption, Carbon 50 (4) (2012) 1583–1590.

[9] Y. Long, M. Śliwińska-Bartkowiak, H. Drozdowski, M. Kempiński, K.A. Phillips, J.C. Palmer, K.E. Gubbins, High pressure effect in nanoporous carbon materials: Effects of pore geometry, Colloids Surf. A 437 (2013) 33–41.

[10] S. Dantas, K.C. Struckhoff, M. Thommes, A.V. Neimark, Pore size characterization of micro-mesoporous carbons using $CO_2$ adsorption, Carbon 173 (2021) 842–848.

[11] M.J. Biggs, A. Buts, D. Williamson, Molecular Simulation Evidence for Solidlike Adsorbate in Complex Carbonaceous Micropore Structures, Langmuir 20 (14) (2004) 5786–5800.

[12] M.J. Biggs, A. Buts, Virtual porous carbons: What they are and what they can be used for, Mol. Simul. 32 (7) (2006) 579–593.

[13] Q. Cai, A. Buts, M.J. Biggs, N.A. Seaton, Evaluation of Methods for Determining the Pore Size Distribution and Pore-Network Connectivity of Porous Carbons, Langmuir 23 (16) (2007) 8430–8440.

[14] C. Lastoskie, K.E. Gubbins, N. Quirke, Pore size distribution analysis of microporous carbons: A density functional theory approach, J. Phys. Chem. 97 (18) (1993) 4786–4796.

[15] A.V. Neimark, Y. Lin, P.I. Ravikovitch, M. Thommes, Quenched solid density functional theory and pore size analysis of micro-mesoporous carbons, Carbon 47 (7) (2009) 1617–1628.

[16] J. Jagiello, J.P. Olivier, Carbon slit pore model incorporating surface energetical heterogeneity and geometrical corrugation, Adsorption 19 (2) (2013) 777–783.

[17] S.M.P. Lucena, J.C.A. Oliveira, D.V. Gonçalves, P.F.G. Silvino, S. Dantas, A.V. Neimark, Pore size analysis of carbons with heterogeneous kernels from reactive molecular dynamics model and quenched solid density functional theory, Carbon 183 (2021) 672–684.

[18] J.C. Palmer, J.K. Brennan, M.M. Hurley, A. Balboa, K.E. Gubbins, Detailed structural models for activated carbons from molecular simulation, Carbon 47 (12) (2009) 2904–2913.

[19] A.H. Farmahini, S.K. Bhatia, Hybrid Reverse Monte Carlo simulation of amorphous carbon: Distinguishing between competing structures obtained using different modeling protocols, Carbon 83 (2015) 53–70.

[20] S. Furmaniak, A.P. Terzyk, P.A. Gauden, P. Kowalczyk, P.J.F. Harris, The influence of the carbon surface chemical composition on Dubinin-Astakhov equation parameters calculated from $SF_6$ adsorption data – grand canonical Monte Carlo simulation, J. Phys.: Condens. Matter 23 (39) (2011) 395005.

[21] J.C. Palmer, A. Llobet, S.H. Yeon, J.E. Fischer, Y. Shi, Y. Gogotsi, K.E. Gubbins, Modeling the structural evolution of carbide-derived carbons using quenched molecular dynamics, Carbon 48 (4) (2010) 1116–1123.

[22] M.W. Thompson, B. Dyatkin, H.-W. Wang, C.H. Turner, X. Sang, R.R. Unocic, C.R. Iacovella, Y. Gogotsi, A.C.T. Van Duin, P.T. Cummings, An Atomistic Carbide-Derived Carbon Model Generated Using ReaxFF-Based Quenched Molecular Dynamics, C 3 (4) (2017) 32.

[23] N.A. Marks, Generalizing the environment-dependent interaction potential for carbon, Phys. Rev. B 63 (3) (2000) 035401.

[24] C. de Tomas, I. Suarez-Martinez, F. Vallejos-Burgos, M.J. López, K. Kaneko, N.A. Marks, Structural prediction of graphitization and porosity in carbide-derived carbons, Carbon 119 (2017) 1–9.

[25] C. de Tomas, I. Suarez-Martinez, N.A. Marks, Carbide-derived carbons for dense and tunable 3D graphene networks, Appl. Phys. Lett. 112 (25) (2018) 251907.

[26] T.B. Shiell, D.G. McCulloch, D.R. McKenzie, M.R. Field, B. Haberl, R. Boehler, B.A. Cook, C. de Tomas, I. Suarez-Martinez, N.A. Marks, J.E. Bradby, Graphitization of Glassy Carbon after Compression at Room Temperature, Phys. Rev. Lett. 120 (21) (2018) 215701.

[27] J.W. Martin, C. de Tomas, I. Suarez-Martinez, M. Kraft, N.A. Marks, Topology of Disordered 3D Graphene Networks, Phys. Rev. Lett. 123 (11) (2019) 116105.

[28] S.K. Ujjain, A. Bagusetty, Y. Matsuda, H. Tanaka, P. Ahuja, C. de Tomas, M. Sakai, F. Vallejos-Burgos, R. Futamura, I. Suarez-Martinez, M. Matsukata, A. Kodama, G. Garberoglio, Y. Gogotsi, J. Karl Johnson, K. Kaneko, Adsorption separation of heavier isotope gases in subnanometer carbon pores, Nature Commun. 12 (1) (2021) 546.

[29] R. Thyagarajan, D.S. Sholl, A Database of Porous Rigid Amorphous Materials, Chem. Mater. 32 (18) (2020) 8020–8033.

[30] N.J. Corrente, E.L. Hinks, A. Kasera, R. Gough, P.I. Ravikovitch, A.V. Neimark, Modeling adsorption of simple fluids and hydrocarbons on nanoporous carbons, Carbon 197 (2022) 526–533.

[31] F. Rouquerol, J. Rouquerol, K.S.W. Sing, P. Llewellyn, G. Maurin (Eds.), Adsorption by Powders and Porous Solids, second ed., Academic Press, Oxford, 2014, http://dx.doi.org/10.1016/C2010-0-66232-8.

[32] C. de Tomas, I. Suarez-Martinez, N.A. Marks, Graphitization of amorphous carbons: A comparative study of interatomic potentials, Carbon 109 (2016) 681–693.

[33] T.B. Shiell, C. de Tomas, D.G. McCulloch, D.R. McKenzie, A. Basu, I. Suarez-Martinez, N.A. Marks, R. Boehler, B. Haberl, J.E. Bradby, In situ analysis of the structural transformation of glassy carbon under compression at room temperature, Phys. Rev. B 99 (2) (2019) 024114.

[34] F. Vallejos-Burgos, 3D-VIS, 2023, http://dx.doi.org/10.17605/OSF.IO/9HJPW, osf.io/9hjpw.

[35] R.M. Davidson, Molecular structure of coal, in: M.L. Gorbaty, J.W. Larsen, I. Wender (Eds.), Coal Science, Academic Press, 1982, pp. 83–160, http://dx.doi.org/10.1016/B978-0-12-150701-5.50009-7.

[36] J.H. Shinn, From coal to single-stage and two-stage products: A reactive model of coal structure, Fuel 63 (9) (1984) 1187–1196.

[37] P. Burg, D. Cagniant, Characterization of carbon surface chemistry, in: Chemistry & Physics of Carbon, CRC Press, 2007.

[38] R.T. Cimino, P. Kowalczyk, P.I. Ravikovitch, A.V. Neimark, Determination of Isosteric Heat of Adsorption by Quenched Solid Density Functional Theory, Langmuir 33 (8) (2017) 1769–1779.

[39] R. Dash, J. Chmiola, G. Yushin, Y. Gogotsi, G. Laudisio, J. Singer, J. Fischer, S. Kucheyev, Titanium carbide derived nanoporous carbon for energy-related applications, Carbon 44 (12) (2006) 2489–2497.

[40] H. Lee, S.H. Park, S.-J. Kim, Y.-K. Park, K.-H. An, B.-J. Kim, S.-C. Jung, Liquid Phase Plasma Synthesis of Iron Oxide/Carbon Composite as Dielectric Material for Capacitor, J. Nanomater. 2014 (2014) 1–6.

[41] S. Wang, F. Vallejos-Burgos, A. Furuse, Y. Yoshikawa, H. Tanaka, K. Kaneko, The subtracting pore effect method for an accurate and reliable surface area determination of porous carbons, Carbon 175 (2021) 77–86.

[42] S. Wang, F. Tristan, D. Minami, T. Fujimori, R. Cruz-Silva, M. Terrones, K. Takeuchi, K. Teshima, F. Rodríguez-Reinoso, M. Endo, K. Kaneko, Activation routes for high surface area graphene monoliths from graphene oxide colloids, Carbon 76 (2014) 220–231.

[43] J. Rouquerol, P. Llewellyn, F. Rouquerol, Is the BET equation applicable to microporous adsorbents? in: P.L. Llewellyn, F. Rodriguez-Reinoso, J. Rouquerol, N. Seaton (Eds.), Studies in Surface Science and Catalysis, in: Characterization of Porous Solids VII, vol. 160, Elsevier, 2007, pp. 49–56, URL: https://www.sciencedirect.com/science/article/pii/S0167299107800085.

[44] J.W.M. Osterrieth, J. Rampersad, D. Madden, N. Rampal, L. Skoric, B. Connolly, M.D. Allendorf, V. Stavila, J.L. Snider, R. Ameloot, J. Marreiros, C. Ania, D. Azevedo, E. Vilarrasa-Garcia, B.F. Santos, X.-H. Bu, Z. Chang, H. Bunzen, N.R. Champness, S.L. Griffin, B. Chen, R.-B. Lin, B. Coasne, S. Cohen, J.C. Moreton, Y.J. Colón, L. Chen, R. Clowes, F.-X. Coudert, Y. Cui, B. Hou, D.M. D'Alessandro, P.W. Doheny, M. Dincă, C. Sun, C. Doonan, M.T. Huxley, J.D. Evans, P. Falcaro, R. Ricco, O. Farha, K.B. Idrees, T. Islamoglu, P. Feng, H. Yang, R.S. Forgan, D. Bara, S. Furukawa, E. Sanchez, J. Gascon, S. Telalović, S.K. Ghosh, S. Mukherjee, M.R. Hill, M.M. Sadiq, P. Horcajada, P. Salcedo-Abraira, K. Kaneko, R. Kukobat, J. Kenvin, S. Keskin, S. Kitagawa, K.-i. Otake, R.P. Lively, S.J.A. DeWitt, P. Llewellyn, B.V. Lotsch, S.T. Emmerling, A.M. Pütz, C. Martí-Gastaldo, N.M. Padial, J. García-Martínez, N. Linares, D. Maspoch, J.A. Suárez del Pino, P. Moghadam, R. Oktavian, R.E. Morris, P.S. Wheatley, J. Navarro, C. Petit, D. Danaci, M.J. Rosseinsky, A.P. Katsoulidis, M. Schröder, X. Han, S. Yang, C. Serre, G. Mouchaham, D.S. Sholl, R. Thyagarajan, D. Siderius, R.Q. Snurr, R.B. Goncalves, S. Telfer, S.J. Lee, V.P. Ting, J.L. Rowlandson, T. Uemura, T. Iiyuka, M.A. van der Veen, D. Rega, V. Van Speybroeck, S.M.J. Rogge, A. Lamaire, K.S. Walton, L.W. Bingel, S. Wuttke, J. Andreo, O. Yaghi, B. Zhang, C.T. Yavuz, T.S. Nguyen, F. Zamora, C. Montoro, H. Zhou, A. Kirchon, D. Fairen-Jimenez, How Reproducible are Surface Areas Calculated from the BET Equation? Adv. Mater. (2022) 2201502.

[45] B. Coasne, A. Grosman, C. Ortega, R.J.M. Pellenq, Physisorption in nanopores of various sizes and shapes : A Grand Canonical Monte Carlo simulation study, in: F. Rodriguez-Reinoso, B. McEnaney, J. Rouquerol, K. Unger (Eds.), Studies in Surface Science and Catalysis, in: Characterization of Porous Solids VI, vol. 144, Elsevier, 2002, pp. 35–42, http://dx.doi.org/10.1016/S0167-2991(02)80217-8.

[46] S. Shimizu, N. Matubayasi, Surface Area Estimation: Replacing the Brunauer–Emmett–Teller Model with the Statistical Thermodynamic Fluctuation Theory, Langmuir 38 (26) (2022) 7989–8002.

[47] M. Sunaga, T. Ohba, T. Suzuki, H. Kanoh, S. Hagiwara, K. Kaneko, Nanostructure Characterization of Carbon Materials with Superwide Pressure Range Adsorption Technique with the Aid of Grand Canonical Monte Carlo Simulation, J. Phys. Chem. B 108 (30) (2004) 10651–10657.

[48] J.N. Caguiat, D.W. Kirk, C.Q. Jia, Uncertainties in characterization of nanoporous carbons using density functional theory-based gas physisorption, Carbon 72 (2014) 47–56.

[49] T. Zelenka, T. Horikawa, D.D. Do, Artifacts and misinterpretations in gas physisorption measurements and characterization of porous solids, Adv. Colloid Interface Sci. 311 (2023) 102831.

[50] H. Kurig, M. Russina, I. Tallo, M. Siebenbürger, T. Romann, E. Lust, The suitability of infinite slit-shaped pore model to describe the pores in highly porous carbon materials, Carbon 100 (2016) 617–624.

[51] M. Kwiatkowski, V. Fierro, A. Celzard, Confrontation of various adsorption models for assessing the porous structure of activated carbons, Adsorption 25 (8) (2019) 1673–1682.

[52] A. Vishnyakov, P.I. Ravikovitch, A.V. Neimark, Molecular Level Models for $CO_2$ Sorption in Nanopores, Langmuir 15 (25) (1999) 8736–8742.

[53] D. Lozano-Castelló, D. Cazorla-Amorós, A. Linares-Solano, Usefulness of $CO_2$ adsorption at 273 K for the characterization of porous carbons, Carbon 42 (7) (2004) 1233–1242.

[54] S. Dantas, K.C. Struckhoff, M. Thommes, A.V. Neimark, Pore size characterization of micro-mesoporous carbons using CO2 adsorption, Carbon 173 (2021) 842–848.

[55] A.D. Buckingham, R.L. Disch, D.A. Dunmur, Quadrupole moments of some simple molecules, J. Am. Chem. Soc. 90 (12) (1968) 3104–3107, Publisher: American Chemical Society.